RSC Advances

Volume 1 | Number 1 | Jan 2013 | Pages 1–100

RSC Advances

www.rsc.org/advances

ROYAL SOCIETY OF CHEMISTRY

ROYAL SOCIETY OF CHEMISTRY

www.rsc.org/advances

Graphical Abstract

The effects of Cu addition on band gap energy, effective mass, and charge transport properties in *n*-type $\mathrm{Cu}x\mathrm{Bi}_2\mathrm{Te}_3$ composites are presented.

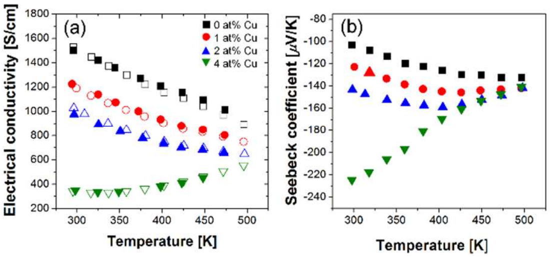

RSC Advances RSCPublishing

ARTICLE

Cite this: DOI: 10.1039/x0xx00000x

Received 00th January 2014,
Accepted 00th January 2014

DOI: 10.1039/x0xx00000x

www.rsc.org/

Effects of Cu addition on band gap energy, density of state effective mass and charge transport properties in Bi_2Te_3 composites

Hyeon Jin Yu,[‡a,b] Mahn Jeong,[‡,a] Young Soo Lim,[*a] Won-Seon Seo,[a] O-Jong Kwon,[c] Cheol-Hee Park,[*,c] and Hae-Jin Hwang[b]

We report the effects of Cu addition on the charge transport properties in *n*-type $Cu_xBi_2Te_3$ composites. The conducting behavior of the composites changed from metallic to semiconducting character with the increase in the amount of Cu, and its origin was found to be the decrease in the electron concentration by the substitution of Bi with Cu. Hall mobilities in the Cu-substituted composites were significantly enhanced due to the alleviated ionized impurity scattering, however, they were governed dominantly by electron-acoustic phonon scattering at relatively high temperature. As well as the carrier concentration and mobility, the electronic structure of Bi_2Te_3 was also affected by the Cu addition, and it was manifested by both the increase in the band gap (~ 198 meV in $Cu_{0.04}Bi_2Te_3$) and the reduction in the density of state effective mass in the Cu-substituted Bi_2Te_3 composites.

Introduction

Since the birth of modern thermoelectrics by Goldsmid, Bi_2Te_3 and its alloyed compounds with Sb and Se have been mostly commercialized for thermoelectric applications due to their very low thermal conductivities (κ), high Seebeck coefficients (S) and high electrical conductivities (σ).[1] Bi_2Te_3 has a rhombohedral structure (R-3m) consisting of three 2D quintuple layers (Te1-Bi-Te2-Bi-Te1).[2,3] The 2D layers are weakly bound to each other by van der Waals force, and the gap between the 2D layers is known to be easy diffusion path for external atoms. Actually, rapid diffusion of Cu atoms through the van der Waals gap has been evidenced by early studies, and electrons can be donated by the intercalated Cu atoms.[4,5] Liu *et al.* reported that the Cu intercalation not only increases the electron concentration, but also reduces the thermal conductivity.[6] Furthermore, reproducibility of *n*-type Bi_2Te_3 composite can also be improved by the reduction of Te-vacancies and also the uncontrollable defect states related to dangling bonds at the grain boundaries.[6] Similar effects has also been reported by Han *et al.*, and the highest thermoelectric figure of merit ($ZT = S^2\sigma T/\kappa$, where T is absolute temperature) of 1.15 has been achieved in $Cu_{0.07}Bi_2Te_3$ at room temperature in their experiments.[7]

Although Cu has been reported as a donor in most studies, there have also been few reports on the *p*-type doping effects of Cu in Bi_2Te_3.[8,9] In this case, Cu atoms locate at Bi-sites rather than the van der Waals gap. Although detailed charge transport properties were not proposed, Cui *et al.* observed the increase of Seebeck coefficient in Cu-doped Bi_2Te_3, which implying the decrease of the electron by Cu-doping.[8] Based on the density functional theory calculations, Chen *et al.* recently reported that the substitution of Cu for Bi is slight easier than the intercalation of Cu into the van der Waals gap.[9] According to their results, Cu acts as both a donor and an acceptor depending on the amount of Cu in Bi_2Te_3. Although Cu is known to be a promising dopant to achieve high ZT in *n*-type Bi_2Te_3, the effects of Cu on the charge transport in Bi_2Te_3 composite has not yet been fully understood as described above.

Herein, we report the charge transport properties in $Cu_xBi_2Te_3$ composites (x = 0, 0.01, 0.02, and 0.04), which prepared by spark plasma sintering. The substitution of Cu for the Bi site was evidenced by Rietveld refinement of X-ray diffraction (XRD) pattern, and it led to the decrease in the electron concentration. As well as the *p*-type doping effect, the increase in the band gap and the reduction in the density of state (DOS) effective mass were observed in the Cu-substituted composites. This results clearly demonstrates that the addition of Cu induces significant modification in the electronic structure of Bi_2Te_3. Also, enhancement of the Hall mobilities was observed in the Cu-substituted composites, and its origin was discussed in terms of the alleviated ionized impurity scattering and the reduced effective mass.

Experimental

Sample preparation

For the preparation of $Cu_xBi_2Te_3$ compounds, raw materials of Cu, Bi and Te were melted in evacuated quartz ampoules by using conventional melting method. Annealing of the prepared ingots was carried out at 663K for 100 h to produce a homogenous Bi_2Te_3 phase. The annealed ingots were pulverized by Spex-mill for 50 min in Ar ambient, and then consolidated by using spark plasma sintering (Well Tech, WT 4000A) under an uniaxial pressure of 60 MPa at 723K for 5 min.

Characterizations of structural and charge transport properties

Powder XRD data were collected at room temperature on a Bragg–Brentano diffractometer (Endeavor D4, Bruker-AXS) with a position sensitive Lynxeye detector and a variable 6-mm divergence slit. Data acquisition covered the angular range $10^o \leq 2\theta \leq 135^o$ at a step width of 0.02° and a total measurement time of 4 h. The structure determination and refinement were performed by using TOPAS software. Microstructural characterizations were also carried out by using a scanning electron microscope (SEM, JSM-6700, JEOL). X-ray photoelectron spectroscopy (XPS) characterization was carried out by using PHI 5000 VersaProbe (ULVAC-PHI) with monochromatic Al Kα x-ray (Figure S1). Temperature-dependent carrier concentration and Hall mobility were characterized by using a high-temperature Hall measurement system (HT-Hall, ResiTest 8300, Toyo). Seebeck coefficient and electrical conductivity were measured by a four probe method using a thermoelectric property measurement system (TPMS, RZ-2001i, Ozawa Science).

Results and discussion

Structural characterization of $Cu_xBi_2Te_3$ composites

Figure 1(a) shows XRD patterns of the sintered bodies of the $Cu_xBi_2Te_3$ composites. Detailed crystal structures of the composites were determined by Rietveld refinement, and the results are summarized in Table 1.

Table 1. Summary of structural information of $Cu_xBi_2Te_3$ composites obtained by Rietveld refinement of XRD patterns.

Cu content (x)	a_o (Å)	c_o (Å)	Bi-Te1 (Å)	Bi-Te2 (Å)	Bi_2TeO_5 (wt%)	R_{wp} (%)
0	4.386(1)	30.48(1)	3.2468	3.0765	1.95	6.18
0.01	4.386(1)	30.49(1)	3.2471	3.0753	2.45	5.94
0.02	4.386(1)	30.49(1)	3.2472	3.0729	2.95	6.37
0.04	4.385(1)	30.51(1)	3.2475	3.0739	1.81	5.86

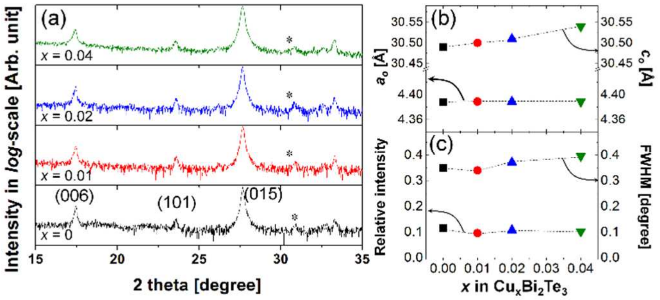

Figure 1. (a) XRD patterns of $Cu_xBi_2Te_3$ composites in *log*-scale intensities. (b) lattice parameters along *a*- and *c*-direction in $Cu_xBi_2Te_3$ composites and (c) relative intensities of (0 0 6) to (0 1 5) peaks and FWHMs of (0 1 5) peaks as a function of x.

They were mainly composed of Bi_2Te_3 phase (JCPDS, No. 15-0863), and Cu_xTe secondary phase[7] was not detected at all even in *log*-scale intensity. However, a small amount of Bi_2TeO_5 phase (denoted by *) was observed in all composites. The lattice parameters along *a*-direction (a_o) were almost constant in the composites, while those along *c*-direction (c_o) increased with the increase in the Cu content as shown in Figure 1(b). In Cu-intercalated Bi_2Te_3 composites, Han *et al*. observed the decrease in the lattice parameter along *c*-direction with increase in the Cu content up to $x = 0.03$.[7] Therefore, this result implies that the Cu atoms are not intercalated into the van der Waals gap, but substituted for the Bi-sites in this experiment. The amounts of Cu at the Bi site were obtained by refining Bi occupancy with constraints of the atomic displacement factors for Bi = Te1 (3a) = Te2 (6c). For compositions with $x = 0$ and 0.01, no significant amounts of Cu were observed. However, it is noteworthy that the Cu occupancy at Bi site was refined as 0.017(7) for $x = 0.02$, and 0.040(8) for $x = 0.04$, respectively. Therefore, Cu atoms preferentially locate at the Bi sites in this experimental condition. In literature, the solubility limit of intercalated Cu in the van der Waals gap was reported to be $x = 0.08$.[7] Although we could not observed the solubility limit of Cu in Bi site, our result shows that the solubility limit should be higher than $x = 0.04$. The role of the substituted Cu atoms is expected to be *p*-type dopant. Furthermore, this substitution of Bi with Cu can lead to the formation of the *p*-type antisite defect of Bi_{Te} due to the cation-excess condition.[10]

Figure 1(c) represents the relative intensity of (006) to (015) peak and also the full width at half maximum (FWHM) of (015) main peaks of the XRD patterns. Both the relative intensities and the FWHMs were not strongly dependent on the amount of Cu in the composites. Furthermore, the average relative intensity was determined to be ~ 0.11 and it was very close to the value (~ 0.10) from the standard powder XRD pattern of Bi_2Te_3. It indicates that the grains in the sintered bodies are almost randomly oriented in the $Cu_xBi_2Te_3$ composites, and that the average grain size is not strongly dependent on the amount of Cu in the composites.

Figures 2(a) ~ (d) are SEM micrographs of the fractured surfaces of the $Cu_xBi_2Te_3$ composites with $x = 0$, 0.01, 0.02, and 0.04, respectively. As expected from the XRD results, the microstructures in the composites were almost identical to each other. Therefore, it is possible to compare the following charge transport properties directly without further consideration on the additional effects of the microstructure.

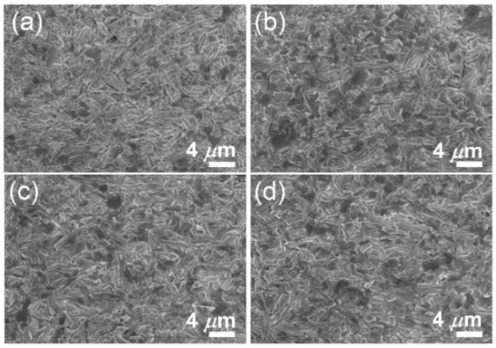

Figure 2. (a) ~ (d) SEM micrographs of the fractured surfaces of the $Cu_xBi_2Te_3$ composites with x = 0, 0.01, 0.02, and 0.04, respectively.

Charge transport properties in $Cu_xBi_2Te_3$ composites

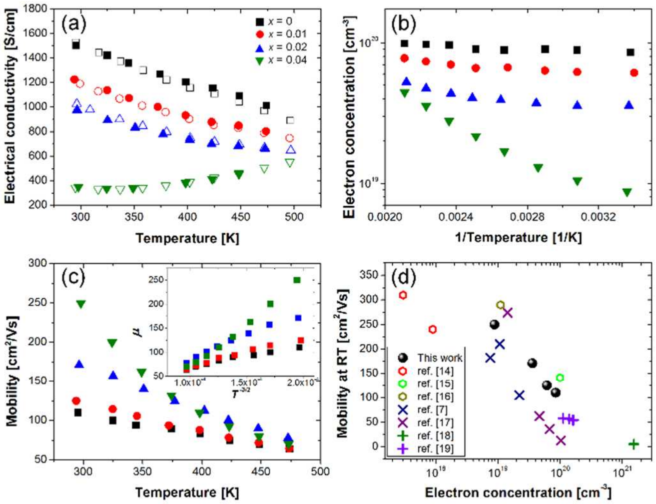

Figure 3. (a) Electrical conductivities of $Cu_xBi_2Te_3$ composites, which characterized by using TPMS (open symbols) and HT-Hall (solid symbols). (b) electron concentrations and (c) Hall mobilities of the composites, which characterized by using HT-Hall. Inset in (c) represents the temperature-dependence of the electron-acoustic phonon scattering in the composites. (d) room-temperature Hall mobilities as a function of carrier concentration (sphere: this work, hexagon: single crystals, x: nanostructured bulk composites, +: thin films).

Temperature-dependent electrical conductivities of the $Cu_xBi_2Te_3$ composites were independently characterized by using TPMS (denoted by open symbols) and HT-Hall measurement (solid symbols), and the results exhibited almost the same tendency as shown in Figure 3(a). As the amount of Cu (x) increases, the electrical conductivity in the composite monotonically decreases and the conducting character changes from metallic to semiconducting. At relatively low Cu content ($0 \leq x \leq 0.02$), the electrical conductivity continuously decreased with the increase in temperature. On the other hand, $Cu_{0.04}Bi_2Te_3$ exhibited positive temperature-dependence in its electrical conductivity. As shown in Figure 3(b), the electron concentrations in the composites, where the metallic conduction was observed (x = 0, 0.01, and 0.02), are not strongly dependent on temperature, indicating that these composites are degenerately doped. It is noteworthy that undoped Bi_2Te_3 exhibited the highest electron concentration among the composites. Because the composites were prepared by the spark plasma sintering of the submicron-sized powder, Te-vacancies can be regarded as the main source for the electrons as proposed by Liu *et al*.[6] Also, because the formation of the second phase (Bi_2TeO_5) can lead to the Te-excess condition slightly,[9] the formation of n-type antisite defect of Te_{Bi} can be the other origin of the high electron concentration in the undoped composite.[11] The electron concentrations in the composites decreased with the Cu addition, and this result is quite consistent with the XRD results, which representing the substitution of Bi with Cu. When x = 0.04, the composite was no longer degenerately doped semiconductor, and the intrinsic carrier concentration exponentially increased with temperature. The band gap energy of the $Cu_{0.04}Bi_2Te_3$ composite, which determined by the intrinsic carrier concentration, was ~ 198 meV, and this value is considerably higher than that of undoped Bi_2Te_3 (~ 130 meV) in literature.[12]

Temperature-dependent Hall mobilities of the $Cu_xBi_2Te_3$ composites are shown in Figure 3(c). The mobilities of the composites were enhanced by the Cu addition, and they were decreasing with increasing temperature due to the electron-acoustic phonon scattering ($\mu \propto T^{-3/2}$) in all composites.[13] As shown in Figure 3(d), it has been reported that the Hall mobility in n-type Bi_2Te_3 decreases with the increase in the carrier concentration at room temperature. It is noteworthy that our result is in a good agreement with the reported values which obtained even from single crystals,[14-16] nanostructured composites,[7,16,17] and thin films.[18,19] Considering Mathiessen's rule for the mobility ($1/\mu = 1/\mu_{ph} + 1/\mu_{ii} + 1/\mu_{gb}$, where μ_{ph}, μ_{ii}, and μ_{gb} are the mobilities governed by phonon scattering, ionized impurity scattering and grain boundary scattering, respectively), this result can only be explained by the ionized impurity scattering.[20] Although the mobility is obviously influenced by the electron-phonon scattering in whole temperature range as shown in Figure 3(c), the mobility in n-type Bi_2Te_3 is also affected by the ionized impurity scattering at relatively low temperature. It can be manifested by the temperature-dependence of the mobility in the inset of Figure 3(c). The mobility slightly deviates from the relation of $\mu \propto T^{-3/2}$ at relatively low temperature due to the influence of the ionized impurity scattering, and this deviation becomes much severe in the composites which containing relatively small Cu content. Therefore, the alleviated ionized impurity scattering can be an origin for the enhancement of the mobility in Cu-substituted Bi_2Te_3 composites.

Seebeck coefficients and DOS effective masses in $Cu_xBi_2Te_3$ composites

Temperature-dependent Seebeck coefficients of the composites are shown in Figure 4(a). The Seebeck coefficient can be expressed by Pisarenko relation in Eq. (1).

$$S = \frac{8\pi^2 k_B^2 T}{3qh^2} m_d^* \left(\frac{\pi}{3n}\right)^{2/3} , \quad (1)$$

where k_B is Boltzmann constant, q is carrier charge, h is Plank constant, m_d^* is the DOS effective mass, and n is the electron concentration. At relatively low temperature, degenerately doped $Cu_xBi_2Te_3$ composites (x = 0, 0.01, and 0.02) exhibited quite linear relationship with temperature due to the almost constant carrier concentration. The linearity diminished at relatively high temperature due to the onset of the bipolar effect. Meanwhile, the Seebeck coefficient of $Cu_{0.04}Bi_2Te_3$ was decreasing with increasing temperature, and it can be explained by the exponentially increasing intrinsic carrier concentration as shown in Figure 3(b).

From the Seebeck coefficient and the carrier concentration, the DOS effective mass, *i.e.*, the effective mass at Fermi level, was estimated by using Pisarenko relation. The slopes of $S{\cdot}n^{2/3}$ vs. T in Figure 4(b) indicate the DOS effective masses in the composites, and they exhibited quite linear relationship with temperature except for x = 0.04.[21] Because Eq. (1) is valid in homopolar semiconductor, the effective mass in $Cu_{0.04}Bi_2Te_3$ could not be exactly deduced due to its intrinsic character.[22] The effective masses in Bi_2Te_3, $Cu_{0.01}Bi_2Te_3$ and $Cu_{0.02}Bi_2Te_3$ were 0.76, 0.64 and 0.47 m_e, respectively. Therefore, the reduction in the effective mass can be the other origin for the enhanced mobilities in the Cu-substituted Bi_2Te_3 composites in Figure 3(c). With these results, it can be concluded that the Cu addition not only affects the electron concentration in the composites, but also induces significant modification in the electronic structure of Bi_2Te_3.

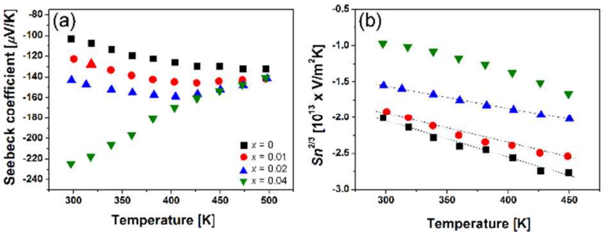

Figure 4. (a) Seebeck coefficients of $Cu_xBi_2Te_3$ composites and (b) A plot of $S{\cdot}n^{2/3}$ vs. T for the estimation of DOS effective masses based on Pisarenko relation.

Conclusions

The effects of Cu addition on the charge transport properties in *n*-type $Cu_xBi_2Te_3$ composites were investigated. The preferential occupation of Bi-sites by Cu atoms were observed by the Rietveld refinement of XRD patterns, however, the microstructures in the composites were not strongly affected by the Cu addition. On the other hand, the charge transport properties in the composites were significantly affected by the substitution of Bi with Cu. Decrease in the electron concentration and increase in the Hall mobility were observed in Cu-substituted composites, and their origin was discussed. Furthermore, significant impacts of the Cu addition on the electronic structure of Bi_2Te_3 were manifested by both the increased band gap energy and the decreased DOS effective masses in the Cu-substituted Bi_2Te_3 composites.

Acknowledgements

This research was supported by Business for Cooperative R&D between Industry, Academy, and Research Institute (No. C0004311) funded by Korea Small and Medium Business Administration, and also supported by Nano·Material Technology Development Program (No. 2011-0030147) through the National Research Foundation of Korea (NRF) funded by the Ministry of Education, Science and Technology, Republic of Korea.

Notes and references

‡H.J. Yu and M. Jeong contributed equally to this work

[a] Energy and Environmental Division, Korea Institute of Ceramic Engineering and Technology, Seoul 153-801, Republic of Korea. E-mail: yslim@kicet.re.kr

[b] LG Chem/Research Park, Daejeon 305-380, Republic of Korea. E-mail: pmoka@lgchem.com

[c] Division of Materials Science and Engineering, Inha University, Incheon 402-751, Republic of Korea.

Electronic supplementary information (ESI) available: XPS characterization of $Cu_{0.04}Bi_2Te_3$. See DOI: 10.1039/b000000x/

1 H.J. Goldsmid, *Brit. J. Appl. Phys*., 1954, **5**, 387.
2. X. Li, H. Ren and Y. Luo, *Appl. Phys. Lett*., 2011, **98**, 083113.
3. F. Zahid and R. Lake, *Appl. Phys. Lett*., 2010, **97**, 212102.
4. R.O. Carlson, *J. Phys. Chem. Solids*, 1960, **13**, 65.
5. T.A. McCarthy and H.J. Goldsmid, *J. Phys. D: Appl. Phys*., 1970, **3**, 697.
6. W.-S. Liu, Q. Zhang, Y. Lan, S.Chen, X. Yan, Q. Zhang, H. Wang, D. Wang, G. Chen and Z. Ren, *Adv. Ener. Mater*., 2011, **1**, 577.
7. M.-K. Han, K. Ahn, H.J. Kim, J.-S. Rhyee and S.-J. Kim, *J. Mater. Chem*., 2011, **21**, 11365.
8. J.L. Cui, L.D. Mao, W. Yang, X.B. Xu, D.Y. Chen and W.J. Xiu, *J. Solid State Chem*., 2007, **180**, 3583.
9. S. Chen, K.F. Cai, F.Y. Li and S.Z. Chen, *J. Electro. Mater*., 2014, **43**, 1966.
10. G.R. Miller and C.-Y. Li, *J. Phys. Chem. Solids*, 1965, **26**, 173.
11. N. Peranio, M. Winkler, M. Dürrschnable, J. König and O. Eibl, *Adv. Funct. Mater*., 2013, **23**, 4969.
12. R. Sehr and L.R. Testardi, *J. Phys. Chem. Solids*, 1962, **23**, 1219.
13. B. R. Nag, *Electron Transport in Compound Semiconductors*; Berlin, Heidelberg, New York: Springer-Verlag, 1980.
14. C.B. Satterthwaite and R.W. Ure, Jr., *Phys. Rev*., 1957, **108**, 1164.
15. R.A. Laudise, W.A. Sunder, R.L. Barns, R.J. Cava and T.Y. Komentani, *J. Cryst. Growth*, 1989, **94**, 53.
16. A.J. Rosenberg and A.J. Strauss, *J. Phys. Chem. Solids*, 1961, **19**, 105.
17. J.S. Son, M.K. Choi, M.-K. Han, K. Park, J.-Y. Kim, S.J. Lim, M. Oh, Y. Kuk, C. Park, S.-J. Kim and T. Hyeon, *Nano Lett*., 2012, **12**, 640.
18. M.-Y. Kim and T.-S. Oh, *J. Electro. Mater*., 2013, **42**, 9.
19. A. Boulouz, A. Giani, F. Pascal-Delannoy, M. Boulouz, A. Foucaran and A. Boyer, *J. Cryst. Growth*, 1998, **194**, 336.
20. B. G. Streetman, *Solid State Electronic Devices*; Englewood Cliffs: Prentice-Hall, 1980.
21. W.H. Nam, Y.S. Lim, S.-M. Choi, W.-S. Seo and J.Y. Lee, *J. Mater. Chem*., 2012, **22**, 14633.
22. D.S. Lee, T.-H. An, M. Jeong, H.-S. Choi, Y.S. Lim, W.-S. Seo, C.-H. Park, C. Park and H.-H. Park, *Appl. Phys. Lett*., 2013, **103**, 232110.